Advances in Comparative Physiology from High-Speed Imaging of Animal and Fluid Motion

George V. Lauder and Peter G.A. Madden

Museum of Comparative Zoology, Harvard University, Cambridge, Massachusetts 02138; email: Glauder@oeb.harvard.edu

Annu. Rev. Physiol. 2008. 70:143–63

First published online as a Review in Advance on September 17, 2007

The *Annual Review of Physiology* is online at http://physiol.annualreviews.org

This article's doi: 10.1146/annurev.physiol.70.113006.100438

0066-4278/08/0315-0143$20.00

Key Words

kinematics, fluid dynamics, video, fluid flow, particle image velocimetry

Abstract

Since the time of Muybridge and Marey in the last half of the nineteenth century, studies of animal movement have relied on some form of high-speed or stop-action imaging to permit analysis of appendage and body motion. In the past ten years, the advent of megapixel-resolution high-speed digital imaging with maximal framing rates of 250 to 100,000 images per second has allowed new views of musculoskeletal function in comparative physiology that now extend to imaging flow around moving animals and the calculation of fluid forces produced by animals moving in fluids. In particular, the technique of digital particle image velocimetry (DPIV) has revolutionized our ability to understand how moving animals generate fluid forces and propel themselves through air and water. DPIV algorithms generate a matrix of velocity vectors through the use of image cross-correlation, which can then be used to calculate the force exerted on the fluid as well as locomotor work and power. DPIV algorithms can also be applied to images of moving animals to calculate the velocity of different regions of the moving animal, providing a much more detailed picture of animal motion than can traditional digitizing methods. Although three-dimensional measurement of animal motion is now routine, in the near future model-based kinematic reconstructions and volumetric analyses of animal-generated fluid flow patterns will provide the next step in imaging animal biomechanics and physiology.

INTRODUCTION

Kinematics: the study of the motion of objects

Humans are visual animals, and many advances in physiology over the past 200 years have come from insights derived from the visualization of structure and function. From Aristotle to da Vinci to van Leeuwenhoek, to Marey, Muybridge, and Ramón y Cajal, to modern biologists advancing visualization technology, many advances in the study of the nervous, circulatory, and musculoskeletal systems have come about through improvements in the visualization of biological structure and the development of methods to visualize physiological function. Techniques such as scanning and transmission electron microscopy, dye visualization of biological tissues, dissection, patterns of gene expression in microarrays, and computer graphic visualization of complex phenomena such as turbulent mixing in the respiratory system all play major roles both in understanding biological systems and in generating new hypotheses for future investigation. Indeed, it is difficult to overstate the significance of simply being able to see structure and function at all levels of biological design.

Although not all biological characteristics are amenable to visual display and analysis, many are. Two such areas of investigation are the examination of animal movement (kinematics) and the study of organismal fluid dynamics. Research in both areas shares the technique of high-speed imaging to reveal motion of either the animal or fluids, and in both fields major advances have occurred in recent years. Since the time of Muybridge and Marey in the last half of the nineteenth century (1, 2), studies of animal motion and the function of the musculoskeletal system have relied on some form of high-speed or stop-action imaging to permit analysis of appendage and body movement (e.g., References 3, 4–8). Stopping the rapid motion of the body, limbs, fins, and wings allows an understanding of the kinematic pattern generated by the nervous system, the dynamics of movement, and the diversity of animal movements generated in response to predators and different physical conditions. The study of organismal fluid dynamics has also benefited greatly from improvements in visualization technology. The newly acquired ability to visualize air and water flow over freely moving animals and in the wake of moving appendages has greatly stimulated comparative investigations of organismal hydrodynamics (9–18) and has facilitated new links to the nascent field of biorobotics (19–24).

In this review, we focus within the arena of comparative animal physiology on the use of high-speed imaging of animal and fluid motion to reveal key features of the locomotor design of animals. Examples are drawn primarily from the field of aquatic locomotion but are broadly applicable to other areas of active research.

TWO ENABLING TECHNOLOGIES

Advances in technology often have unexpected consequences. Biological systems that have been previously studied at one resolution often reveal unexpected complexity at another resolution. This new clarity may give rise to novel ideas about how to analyze data, and from there new hypotheses often arise. New technologies, which may begin and develop in a largely hypothesis-free world of design and engineering, frequently generate wholly new subdisciplines with new ideas and experiments that were never conceived previously.

Two such technological advances have contributed greatly to recent studies of animal kinematics and biological fluid mechanics: high-speed digital video systems and relatively low-cost laboratory lasers. These approaches have roots that go back more than 100 years, but within the past decade advances in these areas have brought both technologies well within the reach of many biological research laboratories, with a consequent expansion of research in organismal kinematics and fluid dynamics. We consider organismal kinematics and fluid dynamics in turn,

discussing for each the technology, data analysis, and what we have learned about organismal function.

High-Resolution, High-Speed Video

Not that long ago, imaging of organismal function was accomplished with movie cameras through the use of film stock that required separate development and a delay, often days, before the sequences taken could be viewed. Nonetheless, considerable progress was made with the use of movie cameras at high framing rates (e.g., References 25 and 26). But progress in understanding how animals move has been increased immeasurably by the advent of digital imaging systems that offer immediate viewing of sequences, despite the low image resolutions in the early digital camera systems. Even as recently as 2002, an image resolution of 480-by-420 pixels at framing rates of 250 Hz was seen as a good-quality video system. Despite the considerable reduction in resolution of digital imaging compared with that of film, the convenience of digital imaging with instant viewing far outweighed the loss of image quality in the first digital systems. In addition, the use of postevent triggering with a circular digital video buffer allowed video capture after an unpredictable animal movement had occurred, greatly improving our ability to study infrequent behaviors compared with the use of high-speed film cameras. But since 2005, a variety of high-speed digital video systems have appeared on the market. These newer systems can obtain images with megapixel (1024-by-1024 pixel) or greater resolution, at framing rates of 1000 Hz and beyond. And video systems with ever-higher resolutions and framing rates are being introduced every few years. Megapixel resolution is beginning to approach the quality of film and allows visualization of details previously lost to low-resolution systems.

The application of megapixel digital video technology to the study of aquatic locomotion can be seen in **Figure 1**, in which imaging of fish fin function allows visualization of each fin ray and its branches as well as details of fin conformational change during locomotion. The pattern of fin deformation in both the spanwise and chordwise directions is clearly visible, and the relative motion of leading and trailing edges of the fins can be distinguished. Other recent applications of high-speed video technology include studies of bird and insect flight (27–30); rapid motion of ant, lobster, and shrimp appendages during sensing and prey capture (31–33); invertebrate locomotion (34); prey capture in fishes (35–37); and fish and lizard locomotion (5, 17, 38–43).

Cross-correlation: in image processing, a procedure by which patterns of pixel intensity are compared, either spatially or through time

Analysis of high-speed imaging data. Analyzing high-speed imaging data is challenging, and a variety of approaches have been tried in recent years. The simplest approach has been to measure the x,y position of individual points in space from a single movie, frame by frame. Such data are calibrated by the filming of a ruler or other flat length scale to allow a pixel-to-real-world length scale conversion, giving a two-dimensional representation of animal movement. However, quantitative three-dimensional calibration using volumetric calibration devices is becoming more common and corrects (linearly) for distortions across the camera field of view. Such direct linear transformation (DLT) calibrations have been used, for example, in studies of bird flight (44), lizard locomotion (45), and fish locomotion (43, 46) as well as in numerous studies on human movement (e.g., Reference 47). The use of DLT for accurate three-dimensional analyses of animal kinematics is greatly improved when multiple cameras are in simultaneous use. When deformation of the animal or appendage is considerable, three or more cameras are needed to provide at least two views of each part of the moving appendage at all times.

An alternative to digitizing multiple individual points is now available and involves the use of an image cross-correlation algorithm. Below we consider the application of image cross-correlation to studies of organismal

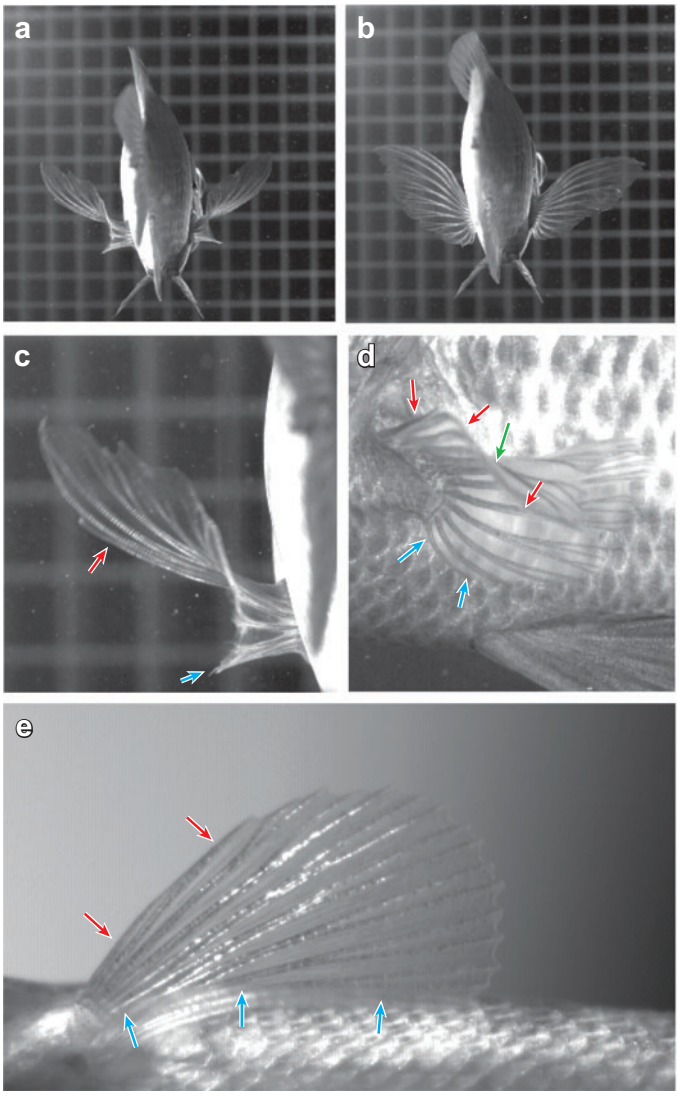

Figure 1

Sample individual video frames from high-speed video (250 and 500 Hz) of fin motion in a freely swimming bluegill sunfish, *Lepomis macrochirus* (*a–d*), and killifish, *Fundulus diaphanus* (*e*), to illustrate high-resolution imaging of a deformable biological propulsive surface. Fish fins are composed of bony segmented fin rays separated by a thin collagenous membrane. With megapixel video resolution, each fin ray is visible, as are the segments within the fin rays and the branches of each ray at the distal end of the fin (5, 17, 18). Images such as these are critical for understanding the function of biological propulsors and the role that flexibility plays in the efficiency of propulsion (62). Panels *a* and *b* show the conformation of the pectoral fin as seen in posterior view (from behind) during the fin outstroke (*a*) and instroke (*b*), whereas panels *c* and *d* show close views of fin conformation from the posterior and lateral (side) views, respectively. Note the "cupped" configuration of the fin as seen in panel *c*, in which both upper (dorsal, *red arrows*) and lower (ventral, *blue arrows*) regions of the fin form two simultaneous leading edges as the fin moves out from the body. Significant deformation of the fin is seen in panel *d*, in which a wave of bending (*green arrow*) passes out the dorsal edge of the fin from the fin base toward the distal (outer) margin. Panel *e* shows a close view of the pectoral fin; the dorsal and ventral margins are indicated by the red and blue arrows, respectively.

fluid dynamics, and here we focus on the use of this technique for the study of animal velocities and accelerations after describing the basic ideas behind image correlation.

Figure 2 illustrates the basic principle of this approach [more details are available in numerous publications that address image analysis in fluid mechanics (48–52)]. Any portion of any image with a pattern can be analyzed by correlation of the pattern of pixel intensities in one subarea of the image with the same (homologous) area at some instant (*dt*) later in time (**Figure 2*a*,*b***). Calculation of the displacement of the correlation peak from zero pixel displacement provides an estimate of the direction of movement of the pattern within that subregion of the image (e.g., **Figure 2*c***).

Some form of patterning with a variety of pixel intensities is needed within each subregion to generate accurate cross-correlation peaks, and in fluid dynamics such a pattern is generated in the fluid by seeding air or water flows with small reflective particles (10, 12, 53–55).

When each subregion of the entire image with a pattern is analyzed, often with 50% overlap among subregions, a matrix of velocity vectors that describes the motion of the patterned elements within the image is produced. For example, **Figure 2*d*** shows an image of the

dorsal fin and tail of a swimming perch illuminated by laser light showing the characteristic speckled pattern of reflections from seeded particles added to the water (56). **Figure 2*e*** shows the matrix of velocity vectors generated by analyzing numerous subregions within the image, and this pattern provides an excellent estimate of the movement of the fluid.

Most usefully for studies of animal kinematics, this cross-correlation approach, developed for studies of fluid mechanics, can also be applied to appropriately patterned images of moving animals. **Figure 3** shows just such an analysis from Danos & Lauder (57), in which the pattern on the body of a zebrafish was analyzed as the fish executed a turning maneuver. The lighting used for these recordings produced a dark background and an illuminated fish that was tracked with image cross-correlation. A distinct center of rotation can be seen over the body between the pectoral fins (**Figure 3*c***), and vectors located at various points on the body can be extracted for further analysis.

Image cross-correlation has the further benefit of avoiding the laborious tasks of digitizing individual points on the body of moving animals and then differentiating these data twice to obtain velocities and accelerations (see References 58 and 59). Because velocity data are obtained directly and overall body velocity results from the averaging of many vectors, accuracy is greatly increased for the measurement of body or appendage acceleration. **Figure 4** shows an analysis of body accelerations resulting from pectoral fin locomotion in a bluegill sunfish. Velocity vectors were calculated for a sequence of images of the fish while it was moving (**Figure 4*a***), and a region of vectors over the center of mass was extracted and averaged to obtain the pattern of body velocity change through time in both the vertical (lift) and front-back (thrust) directions. Integration and differentiation of these data generate displacements and accelerations, respectively.

What have we learned? If we do not know how biological structures move, it is difficult to understand the function of muscles that power movement and the diversity of behaviors performed by animals. Accurate kinematic data now form the basis of most studies on the comparative biomechanics of movement and are foundational for analyses of neural control and pattern generation by the central nervous system. Furthermore, kinematic data are often critical as input into fluid dynamic or mechanical models (3, 32, 60–65) and as such form a crucial step in understanding how animals generate force during movement.

Examples of discoveries from kinematic analyses of animals include

1. prey capture using remarkably fast motions (e.g., References 26, 33, 35, and 37),
2. determining the natural mechanical environment of muscle (e.g., References 20, 60, and 61), and
3. understanding the origin and function of animal limbs, wings, and fins (e.g., References 3, 5, 28, 46, 64, 67, and 99).

Digital imaging in the future. The desire for ever higher framing rates at ever higher resolutions has not abated. Many studies, especially those on insect flight dynamics, could benefit from 2–3-megapixel resolution at framing rates up to and beyond 10,000 fps. Such camera systems will undoubtedly appear within the near future. For studies of larger animals moving in air or on land, for which infrared reflective markers of millimeter size or greater can be attached, automated data acquisition is now becoming more common (66–68). With automatic motion capture, DLT calibration, and the use of numerous cameras stationed around the moving body to see many markers at the same time, digitizing of individual points is effectively eliminated. Data obtained automatically from such markers can also be integrated with three-dimensional models of the skeleton to provide a full visualization of a moving body and

appendages. Integration of digitized data, however obtained, with three-dimensional models of moving elements is an important new direction that will likely develop rapidly as our ability to reconstruct three-dimensional animal geometries improves (69, 70).

Laser Imaging of Fluid Flow Patterns

The availability of relatively low-cost laboratory lasers that biologists can purchase and use with reasonable ease has revolutionized the analysis of the fluid dynamics of animal locomotion. The technique of digital particle image velocimetry (DPIV, often simply termed

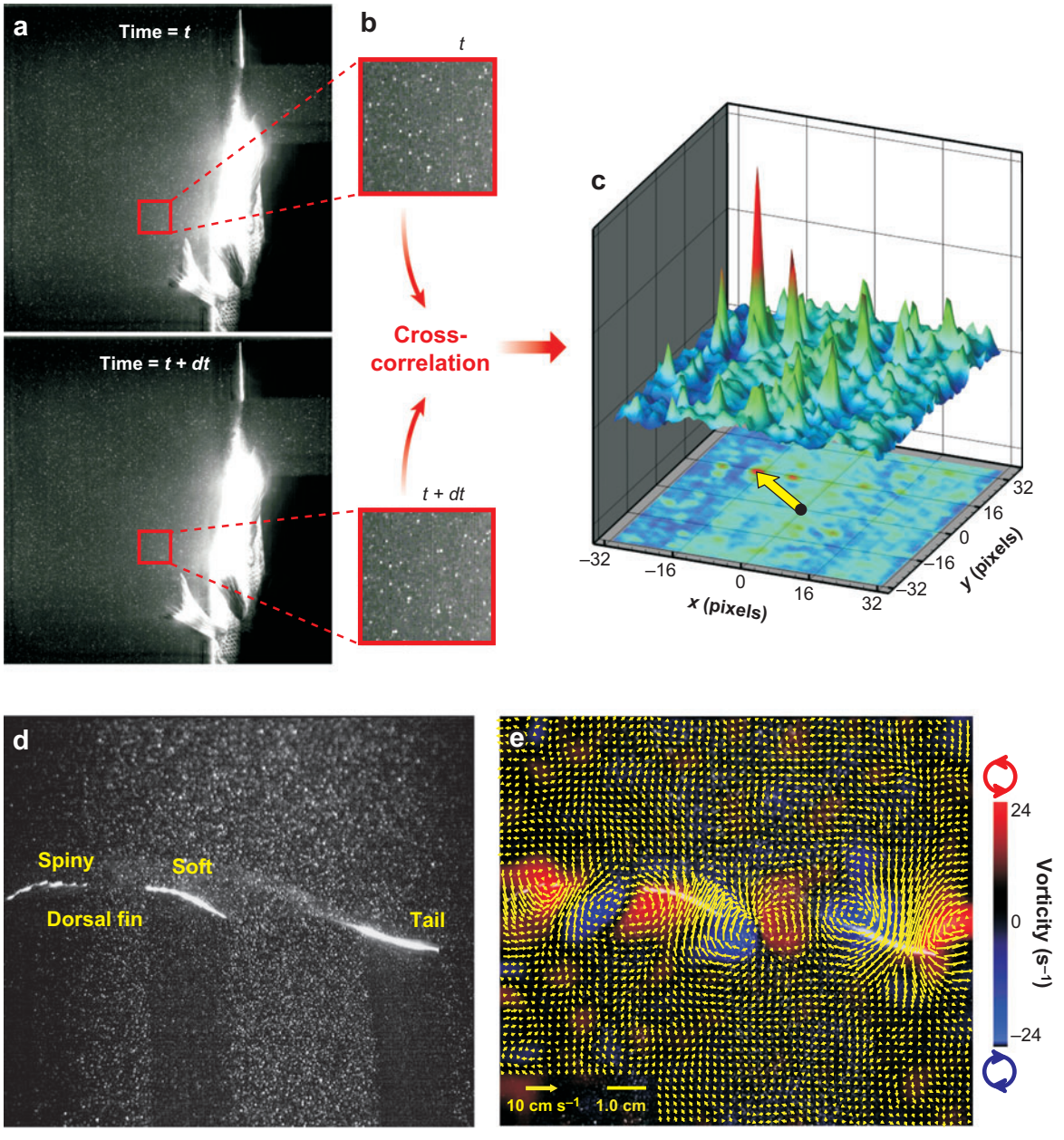

PIV), relies on lasers to produce light to image fluid flow patterns that are then analyzed with image cross-correlation (**Figure 2**). DPIV has allowed comparative physiologists to investigate the dynamics of movement though fluids in ways not previously possible. Flow visualization has for many years been accomplished in a largely qualitative way with dye or smoke trails, and such visualizations have been extremely useful. But the ability to reconstruct patterns of fluid movement around moving animals quantitatively has provided a new approach to the study of organisms moving in fluids by allowing estimates of locomotor force, the testing of biomechanical models of animal function, the validation of computational fluid dynamic models, and experimental study of the functional significance of the diversity of organismal shapes and sizes.

Two basic methods for data acquisition. The analytical methodology of DPIV is described above (**Figure 2**) in relation to images to which cross-correlation techniques can be applied. Analysis of fluid flow requires laser illumination of small (1–20 μm) particles introduced into the fluid. Two basic types of lasers have been used for studies of biological fluid dynamics.

First, argon-ion lasers with up to 10 W of power, which generate a continuous laser beam, have been used with good success to generate thin (1–2 mm thick) sheets of light for studies of aquatic locomotion (4, 53, 55, 71–74). Optics of various kinds are used to spread the beam out into a light sheet, and organisms are induced to move their body or appendages either in the laser light sheet or in front of the light sheet so that fluid flow induced by movement can be visualized. Because continuous lasers produce light without interruption, standard high-speed digital cameras can be used to film particle motion in the light sheet. **Figure 5** shows a variety of experimental arrangements of continuous laser light sheets and high-speed video used for studies of swimming fishes. Either one light sheet or two simultaneous light sheets (generated by two lasers) can be used with one-or-more-megapixel digital high-speed cameras to image flow at different locations on a swimming fish (**Figure 5*a***). The laser beam may be scanned through a volume occupied by the moving animal (**Figure 5*b***), producing a more three-dimensional image of flow.

Digital particle image velocimetry (DPIV): the use of image cross-correlation on digital images containing patterns of fluid motion (produced by seeding the fluid with reflective particles) to generate a matrix of velocity vectors

PIV: particle image velocimetry

Figure 2

Image cross-correlation is a useful technique for analyzing patterns of fluid flow and animal movement. Images of animals moving in a fluid seeded with small reflective particles and illuminated by a laser light sheet provide the raw data for digital particle image velocimetry (DPIV) analyses. Panel *a* shows two ventral views of a bluegill sunfish (*Lepomis macrochirus*). Sunfish swam in a laser light sheet that illuminated particles in the flow downstream of the fins (see also **Figure 5**). High-speed video was used to capture a pair of images separated in time by *dt* (typically ranging from 10 μs to 5 ms). These images are subjected to image cross-correlation (*b*) at individual subregions (often sized from 64 by 64 pixels to 8 by 8 pixels) within the image. The red boxes in *a* and *b* show the 32-by-32-pixel subregion subjected to cross-correlation in this example. Cross-correlation for each subregion generates a plot of the magnitude of the correlation (*c*) for each pixel of the subregion, shown as a surface plot in which higher peaks indicate stronger correlations. The yellow vector stretches from the zero-zero point on the *x*-*y* plane of the 32-by-32-pixel image subregion (*black dot*) toward the red dot, which is the projection of the highest peak onto the *x*-*y* plane; peak heights are in arbitrary units. When such analyses are repeated across the full image, a matrix of velocity vectors is generated. Panel *d* shows a full image from a video of a perch (*Perca flavescens*) executing a yawing turn in which the laser light sheet illuminates the two regions of the dorsal fin and tail and particles in the water. Panel *e* shows the vector matrix (*yellow arrows*) that results from a cross-correlation analysis of this image and another analysis 4 ms later. Fluid vorticity is color coded to indicate rotation of the fluid induced by motion of the dorsal fin and tail. Panels *d* and *e* are modified from Reference 56, with permission. **Figure 6** describes calculations from the velocity vector matrix in more detail.

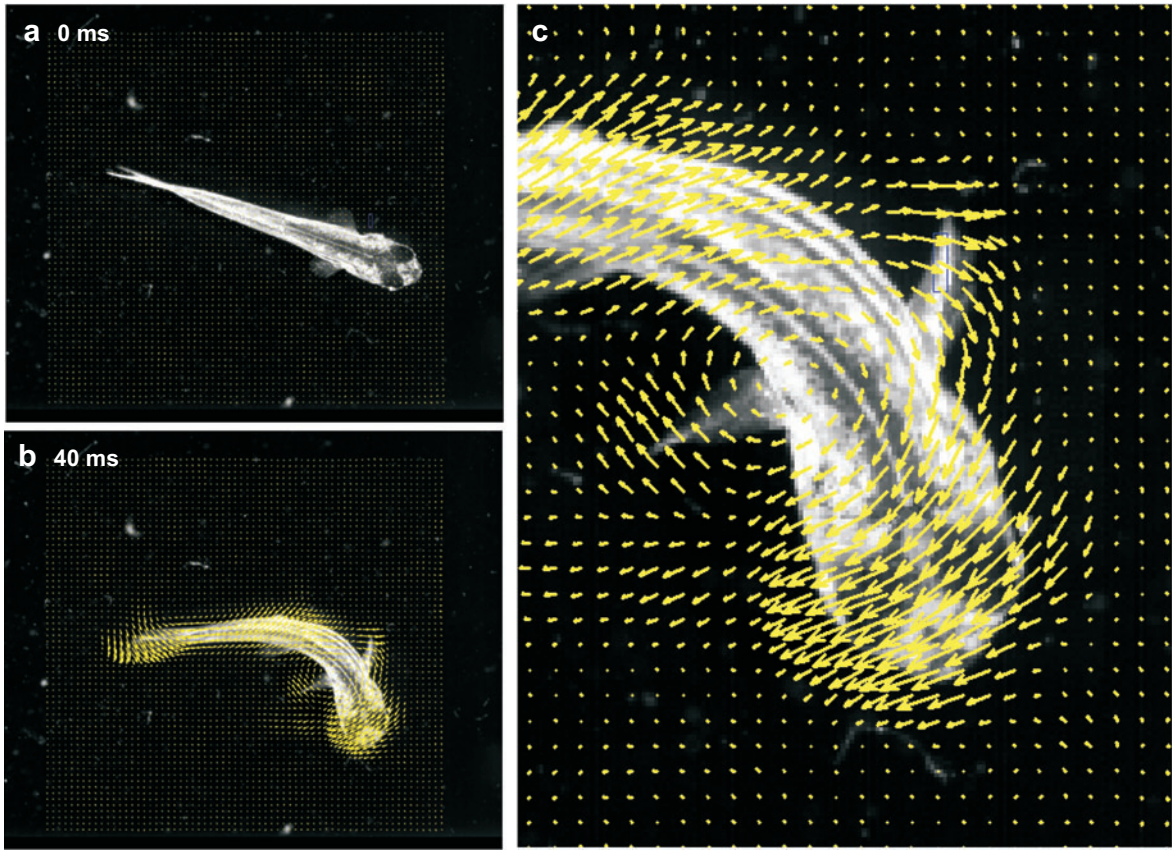

Figure 3

High-speed video images of zebrafish (*Danio rerio*) executing a routine turn. Panels *a* and *b* show the position of the zebrafish at the start of a turn and 40 ms later, respectively. These images are analyzed with image cross-correlation to calculate the velocity of the moving animal. Image cross-correlation tracks the movement of patterns on animals as well as particle displacements in fluid flows, as described in **Figure 2**. A magnified view of the head of the zebrafish in panel *b* is shown in panel *c*. Cross-correlation analysis provides velocity vectors that effectively cover the animal and allow tracking of regional differences in movement. For example, in panel *c*, clockwise rotation of the head and body of the zebrafish and the center of rotation over the base of the right pectoral fin at this point in time can be clearly seen. Small regions of vectors from various points on the body are extracted for further analysis. Modified from Reference 57, with permission.

Another approach is to orient the light sheet in a transverse direction to the moving animal (**Figure 5*c***) and take high-speed images via mirrors behind the animal to quantify flow moving orthogonal to the light sheet (5, 18). If appropriate filters are used with multiple cameras, accurate images of animal position can be obtained with red light; at the same time, stereo images of flow through the transverse light sheet can be obtained with two DPIV cameras that are filtered to see the green laser light reflections (**Figure 5*c***; 18).

The second, and still most commonly used, approach to DPIV is to employ a pulsed laser that generates very short (down to 10 ns) high-energy pulses of laser light but with relatively low frequency (images are captured in pairs at 1–30 Hz). When flow is very fast [10–15 m s^{-1}, for example, as when flying birds or bats are studied (10, 12, 75)], lasers with considerable

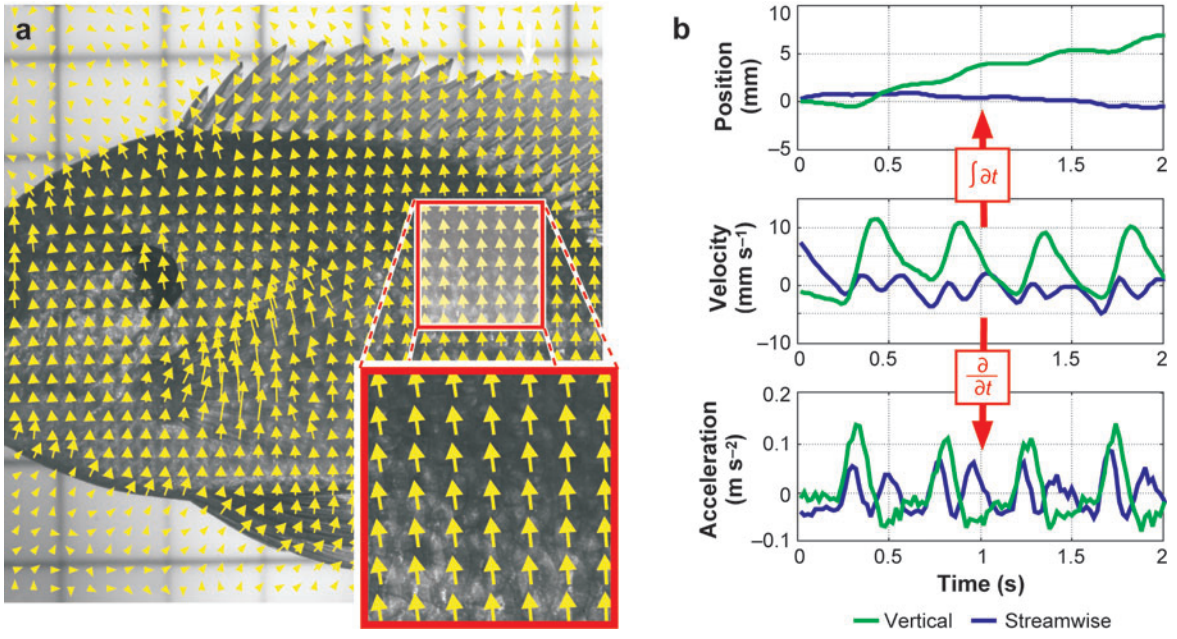

Figure 4

The use of image correlation to analyze body motion during locomotion. Image correlation (see **Figure 2**) is applied to each frame of a high-speed video of pectoral fin locomotion in a bluegill sunfish, and a matrix of velocity vectors is calculated for the whole image, the background, and the moving animal. Panel *a* shows a sample frame. Vectors calculated over the body of the animal reflect the velocity of the moving body at that time. A region of the images that accurately reflects body motion only (*red box*) is selected, and the mean of all velocity vectors in this region is calculated from a series of these images; this shows body velocity through time (*b*). If velocity vectors over a region of the body (*red box*) are averaged and image correlation is used to calculate velocity directly, only one differentiation and integration step is needed to give the acceleration and position, respectively, of the body. [This contrasts with errors that are introduced by manual digitization of one point on the body followed by double differentiation to calculate acceleration (107).] In this case, a double acceleration peak can be seen in the direction of body motion, indicating that the fish accelerates on both the outstroke and return stroke of the pectoral fin (5, 62).

power are needed to illuminate the rapidly moving particles. Specialized digital cameras are synchronized with the laser pulses to obtain image pairs of the moving fluid. The short time exposure is excellent at capturing rapid motion, but with such low frequencies of sampling, a long time series of continuous images that accurately samples fast motions cannot be obtained. Rather, multiple snapshots taken at different times are used to reconstruct the flow pattern.

Once images of particles moving in the fluid are obtained, analysis by image cross-correlation, as described above, provides a matrix of velocity vectors (e.g., **Figure 2*e***) that leads to numerous useful analytical steps. The size of the velocity vector matrices has increased dramatically in recent years as the resolution of high-speed digital cameras has approached one megapixel, and the increase in number of vectors allows much greater resolution in reconstructing fluid flow patterns. Early analyses with lower-resolution video cameras (55) generated matrices of 20 by 20 vectors (400 total vectors), but it is now routine to calculate 175 by 175 vectors (30,625 total vectors) per pair of megapixel images. For a 1000-Hz high-speed digital

video of wake flow around a swimming fish, for example, analysis of a behavior lasting 1 s would generate a data set of a little more than 15.3 million vectors (500 image pairs times approximately 30,000 vectors per pair).

Image cross-correlation DPIV analysis is so useful because the vector matrix provides a wealth of information on locomotor dynamics. **Figure 6** summarizes a selected set of useful calculations that can be completed once the velocity vector field has been estimated. Determining the geometry of fluid motion allows analysis of vortex rings generated by moving animals (12, 42, 55, 56, 76), quantification of fluid rotation (vorticity), vortex strength (circulation), and fluid momentum that results

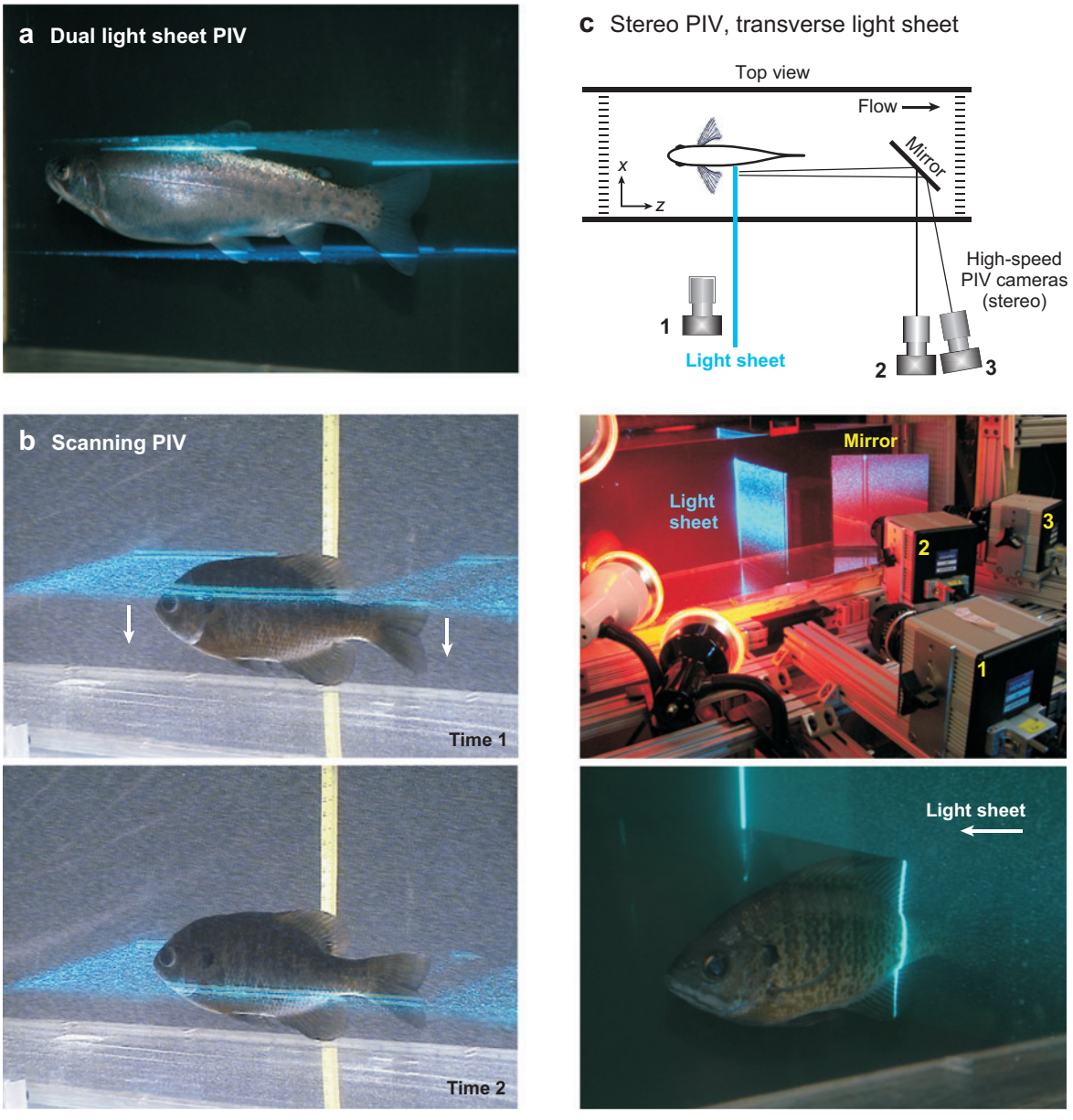

from animal motion as well as force, work, and power. These are quantities that are much more easily calculated for terrestrial locomotor systems in which animals step on force plates, but for aquatic or aerial systems, DPIV is needed to allow estimates of the kinetics of locomotion.

Although DPIV is most often used as a two-dimensional technique that gives information on the flow in a single thin sheet of light, if a separate set of experiments is conducted, reorientation of light sheet orientation can provide some three-dimensional information on flow patterns that allows an estimation of different force components as shown in **Figure 6** (55). However, stereo DPIV is a modification of standard DPIV methods that uses two cameras in a stereo configuration to estimate the out-of-plane flow component directly (18, 77, 78). If a transverse light sheet is used as shown in **Figure 5*c*** in combination with stereo DPIV techniques, a good estimate of all three vector components of flow can be obtained. Data from such an experiment are shown in **Figure 7**, which illustrates velocity vectors in the x, y, and z directions. Such data begin to approach a fully three-dimensional reconstruction of fluid flows generated by organisms.

Another modification of standard DPIV techniques that can be used to increase the three-dimensionality of the data is to rapidly scan the light sheet through a volume of flow in the wake of a moving animal (18, 79). Data shown in **Figure 8** were obtained with the scanning procedure illustrated in **Figure 5*b*** and demonstrate the fluid flow produced by the pectoral fin of a swimming bluegill sunfish at two different times in the fin beat cycle. The vortical structure produced by the fin in the fluid can be seen clearly with two counter-rotating centers of flow.

Tips for success with experiments and analysis. DPIV experiments can be tricky to set up initially, and several problems can crop up to make data analysis and interpretation difficult. Here we provide several tips that we

Velocity vector field: the result of a cross-correlation analysis on images of moving fluid or animals to produce a matrix of velocity vectors that reflect movement

Vorticity: local fluid angular velocity (strictly, the curl of fluid velocity)

Kinetics: the study of the effect of forces on the motion of objects

Figure 5

Imaging fluid flow with digital particle image velocimetry (DPIV) requires illumination of the flow around the body and moving appendages. This is typically accomplished with argon-ion lasers and with optics to spread the laser beam into a thin (1–2 mm) light sheet that is projected toward the moving animal. Panel *a* shows a brook trout swimming between two light sheets produced by two continuous-wave argon-ion lasers to study the function of dorsal and anal fins. High-speed digital video cameras image the fin wake flow patterns simultaneously from above and below. Image by E. Standen, from Standen & Lauder (43), with permission. Panel *b* shows a modification of the DPIV technique: A laser light sheet is scanned through the moving animal to image the fluid wake dynamically and provide a more three-dimensional picture of flow patterns. Still frames from two times during the scan are shown. Flow in the plane of the laser light sheet is imaged from below. Panel *c* shows the experimental arrangement of high-speed cameras used to image flow patterns in a stereo configuration, providing an estimate of all three directional components of flow velocity: x, y, and z. Shown is an example of the experimental arrangement for stereo PIV through the use of a light sheet transverse to swimming bluegill, downstream of the beating pectoral fin. The top panel of *c* shows a schematic top view of the experimental arrangement of cameras and the swimming fish. The use of three high-speed cameras allows simultaneous imaging of body and fin position (camera 1) and stereo DPIV of flow through the transverse light sheet (*top panel*, camera 2 and 3). These two cameras were aimed at a mirror downstream of the swimming fish, imaging at 500 Hz, 1/2000-s shutter speed, and provided data on the u, v, and w components of flow through the transverse laser light sheet. The middle panel of *c* shows the three cameras, the mirror in the flow tank, and the projected transverse laser light sheet. Filters on the cameras allowed kinematic data to be obtained through the use of red light and camera 1, filtering out green laser light. In contrast, only green laser light was seen by cameras 2 and 3, which imaged flow in the laser light sheet. The bottom panel of *c* shows a bluegill swimming in the flow tank; the transverse light sheet is visible as the sheet meets the side of the body. The image in the bottom panel of *c* is courtesy of E. Tytell. Modified from Reference 18, with permission.

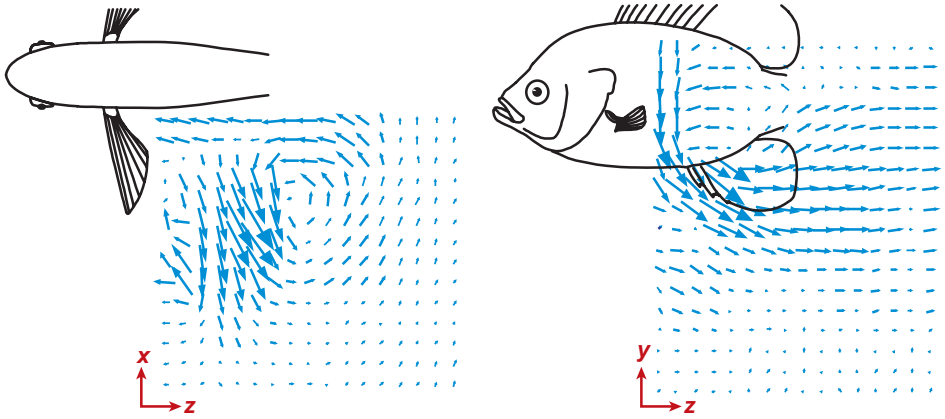

Figure 6

Schematic wake flow patterns behind the pectoral fin of a bluegill sunfish (*Lepomis macrochirus*) as seen in the top view (*left panel*; *x*, *z* axes) and side view (*right panel*; *y*, *z* axes). Velocity vectors calculated with image cross-correlation (**Figure 2**) are shown as a matrix of blue arrows that reflect patterns of local flow velocity induced by fin motion. Once the velocity of induced flow is estimated with image cross-correlation, a wide range of quantities important for the study of aquatic locomotion can be calculated from velocity vector matrices: vorticity, a measure of fluid angular velocity; circulation, a measure of vortex strength; momentum, equal to the density of water times the vortex circulation times the area of the vortex ring (13, 53, 55); three components of force, in Newtons, equal to fluid momentum divided by the time of the fin beat, partitioned into components by analyzing the direction of the main fluid momentum jet in the center of the vortex ring in both the *xz* and *xy* planes; work, in Joules, equal to the force times the distance moved during the fin beat; and power, in Watts, equal to the work divided by the time of the fin beat.

hope will be useful for biologists who might be contemplating using the DPIV approach to quantify flows around their organisms.

First, DPIV need not be expensive. Although expenses for high-power lasers with cooling systems and megapixel high-speed digital cameras can indeed add up, successful experiments have been conducted with laser pointers and camcorders in aquatic systems (80). Analysis packages to perform image cross-correlation are available for free on the Internet as Matlab code, and they do basic analysis functions well.

Second, test your system against a known flow or simple model (81). Imaging fluid flow around a flat plate, cylinder, boundary layer (which has a very well-developed body of theory), or fixed wing of known profile (and hence lift and drag characteristics) will give confidence that the velocity vectors and forces that you calculate are reasonable.

Third, it is critical to view flow images carefully to look for the major flow features. The human eye is very good at picking out patterns in movies of flowing particles, and these patterns should correspond generally to those seen in the analyzed vector fields.

Fourth, control the movement of the animal as best you can (using flow tanks, wind tunnels, or special lighting patterns) to obtain

repeatable behaviors that show similar flow patterns. Use multiple individuals because there can often be substantial differences in behavior among individuals.

Fifth, it is best to use multiple high-speed cameras, if they are available, to know exactly where the animal is relative to the laser light sheet. Too many published studies use only a single camera, and the position of the animal relative to the sheet is not known, greatly complicating the analysis of flow patterns.

There is a very large literature on DPIV that addresses technical issues of particle density, size of image correlation windows, deformation of correlation windows, and temporal sampling of flows of different velocity (e.g., References 51, 52, 82, 83). Biologists should be aware that commercial DPIV software has an almost overwhelming number of parameters that can be adjusted and that the best teacher will be practice in analyzing cannonical flow situations, combined with judicious reading within the extensive literature. From the biological perspective of comparative physiology and biomechanics, key recent issues of interest to researchers using DPIV are (*a*) new methods for calculating locomotor forces through the use of velocity vector data (18, 84, 85) and (*b*) the use of multiple laser light sheets and methods such as laser scanning and stereo DPIV to begin to approach a more three-dimensional view of flow patterns (18, 77).

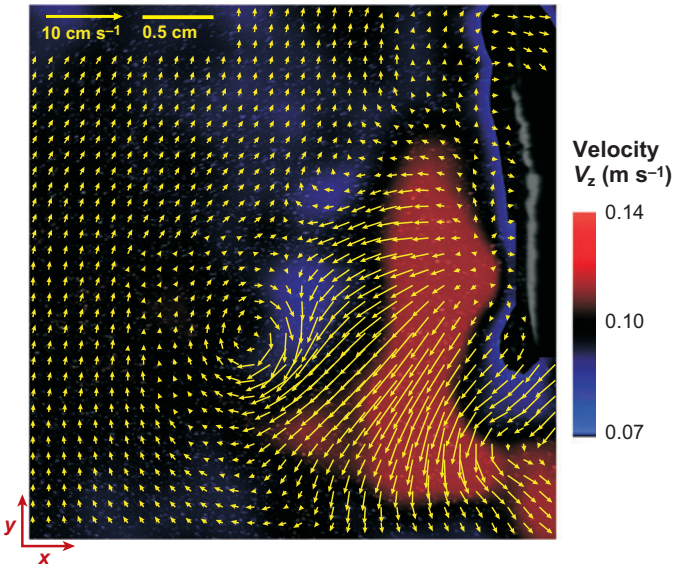

Figure 7

Sample data from a stereo DPIV analysis of fluid flow in the wake of the pectoral fin of a swimming bluegill sunfish. These data were obtained through the use of the experimental arrangement illustrated in **Figure 5*c*** and represent the flow shed by the pectoral fin as seen looking upstream at the wake at a time when the pectoral fin has just completed the outstroke. Velocity vectors are shown for the *x*-*y* plane (representing the *u* and *v* components of flow), and the third (*z*) dimension velocities are represented as background color (showing the *w* component, orthogonal to the plane of the figure). Red color denotes water moving faster than mean free-stream flow (9 cm s^{-1}) as a result of pectoral fin motion, whereas blue indicates flow slowed to less than free stream. The tail extends toward the camera in the middle right of the image, and vectors near the tail have been deleted. The large region of red indicates that the pectoral fin outstroke has accelerated water in the wake to beyond free-stream velocity. Modified from Reference 18, with permission.

What have we learned? Analyses of fluid flows around swimming and flying animals have led to a much more complete understanding of how unsteady fluid forces are generated and manipulated by moving organisms. Key insights include understanding the effects of changes in Reynolds number on locomotor performance (86, 87), clarifying the role of leading-edge vortices in propulsive force generation (14, 88), understanding how animals use multiple propulsive surfaces at the same time to balance locomotor forces (43, 74, 89), understanding the limits of locomotor performance and the fluid dynamic basis of gait change and maneuvers (71, 90, 91), demonstrating how flexible biological propulsive surfaces compare with rigid engineered foils (5, 62), documenting vortex wake patterns and how animals track these patterns through the fluid (10, 12, 55, 75, 80, 92, 93), and using DPIV to test aerodynamic models of lift generation (94, 95). In addition, DPIV has proven to be a very useful adjunct to the use of biorobotic models (14, 17, 96) and allows flows generated by computer-controlled robotic devices to be compared with those produced in vivo by moving animals.

Examples of recent discoveries from hydrodynamic analyses of animals include

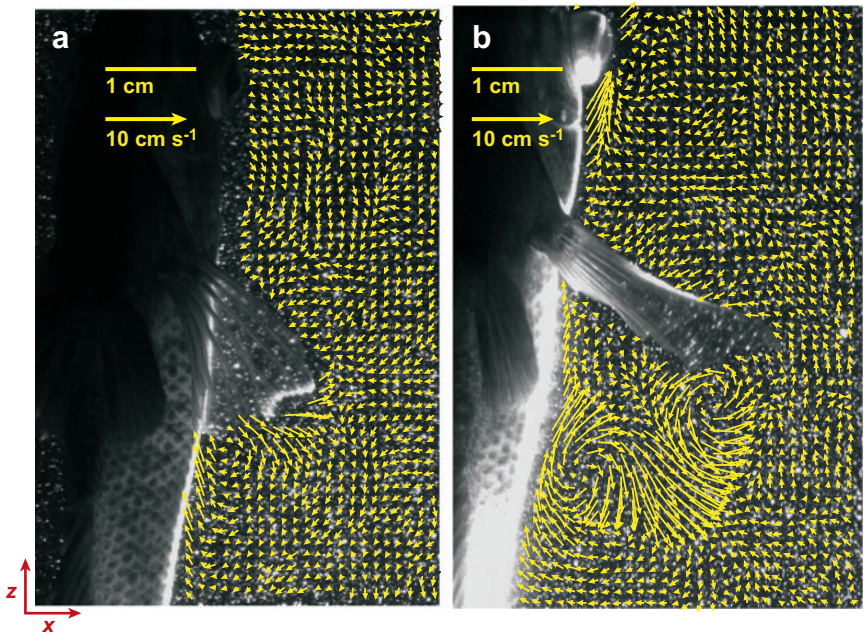

Figure 8

Sample data from a scanning DPIV analysis of fluid flow in the wake of the pectoral fin of a swimming bluegill sunfish. Yellow arrows show the velocity field. A laser light sheet was scanned through a swimming bluegill sunfish to reveal the fluid dynamic wake generated by the pectoral fin as shown in **Figure 5*b***. The laser light sheet scanned from the top to the bottom of the fish, and wake flows were imaged from below at 500 Hz. Images show the wake flow patterns early in the fin outstroke (*a*) and at the transition from outstroke to instroke (*b*). Mean free-stream flow has been subtracted. Modified from Reference 18, with permission.

1. understanding how insect wings generate forces for flight (e.g., References 13, 14, and 96),
2. the diverse vortex wakes of swimming and flying animals (e.g., References 10, 12, 42, and 55),
3. how fins or wings in series can interact hydrodynamically and increase thrust (e.g., References 42, 43, and 73), and
4. testing the predictions of fluid dynamic models (e.g., References 62, 63, 94, and 95).

THE FUTURE OF KINEMATIC AND FLOW IMAGING

Organism-level imaging is in the midst of a tremendous growth period, and new technologies are being developed almost every year. The future of organismal imaging lies in two directions: the extension of both kinematic and fluid dynamic visualization into three dimensions, and three-dimensional visualization of internal movements using X-ray or high-energy beam imaging.

The ability to perform three-dimensional volumetric fluid imaging (termed tomographic PIV) with the entire flow volume measured at one time, and then to track changes in volumetric flows through time, is now becoming reality (97; see also 98). Studies of animal kinematics are also moving increasingly into three dimensions, not only with the use of multiple high-speed cameras to track individual points in the x, y, and z dimensions (3, 44, 99), but also with the construction of three-dimensional models of the animal or its skeleton and then animation of the model's

motion on the basis of the animal's measured movements (69, 70).

The ability to view the motion of internal elements in animals has been accomplished with X-ray cinematography (100–104) and, more recently, with X-ray synchrotron imaging (105, 106). Both approaches have provided important new information on the mechanics and physiology of animals, and such internal visualizations will undoubtedly become ever more important in the future, especially as X-ray imaging evolves to use multiple simultaneous X-ray sources and the reconstruction of three-dimensional motions inside animals.

SUMMARY POINTS

1. Since the time of Muybridge and Marey in the last half of the nineteenth century, studies of animal movement have relied on some form of high-speed or stop-action imaging to permit analysis of appendage and body motion.
2. The advent, within the past ten years, of megapixel-resolution high-speed digital imaging with maximal framing rates of 250 to 100,000 images per second has allowed new approaches to studying musculoskeletal function in comparative physiology that now extend to imaging flow around moving animals and calculating fluid forces produced by animals moving in fluids.
3. Image cross-correlation algorithms as employed by digital particle image velocimetry (DPIV) analyses are a useful method for analyzing patterns of both animal and fluid motion and are the primary means by which fluid flow patterns in the wake of moving animals are estimated.
4. A diversity of vortex wakes generated by swimming and flying animals has now been described through the use of DPIV, and calculations based on the velocity vector fields allow an understanding of the mechanisms of force generation used by animals during feeding, swimming, and sensing in fluid environments.
5. New DPIV techniques such as scanning DPIV and transverse light sheet DPIV provide near-three-dimensional views of fluid flow patterns generated by moving animals.

FUTURE ISSUES

1. High-speed digital cameras will continue to improve in resolution and framing rate, making studies of rapid organismal movements and induced fluid flows ever more feasible.
2. Current two-dimensional analyses of organismal fluid dynamics using digital particle image velocimetry (DPIV) will increasingly give way to techniques that provide three-dimensional information such as scanning DPIV, time-resolved stereo DPIV, and pseudovolumetric analyses that use laser light sheets oriented transversely to free-stream flow.
3. Volumetric analyses that permit full three-dimensional instantaneous capture of fluid flows generated by moving organisms will become routine within the next ten years.
4. Analysis of kinematic data on moving organisms will increasingly use model-based approaches that animate three-dimensional models of organismal anatomy based on measured kinematics.

DISCLOSURE STATEMENT

The authors are not aware of any biases that might be perceived as affecting the objectivity of this review.

ACKNOWLEDGMENTS

The research reported here was supported by an ONR-MURI grant N00014-03-1-0897, monitored by Dr. Thomas McKenna and initiated by Dr. Promode Bandyopadhyay, and by NSF grant IBN0316675 to G.V.L. We thank Drs. Rajat Mittal, Promode Bandyopadhyay, Eliot Drucker, Wolf Hanke, Nicole Danos, and Brooke Flammang for many helpful discussions on bio-inspired propulsion and for collaboration on experiments. Tony Julius provided invaluable assistance in the laboratory.

LITERATURE CITED

1. Braun M. 1992. *Picturing Time. The Work of Etienne-Jules Marey (1830–1904)*. Chicago: Univ. Chicago Press
2. Muybridge E. 1887. *Muybridge's Complete Human and Animal Locomotion*. New York: Dover Publ. Reprint
3. Hedrick TL, Tobalske BW, Biewener A. 2002. Estimates of circulation and gait change based on a three-dimensional kinematic analysis of flight in cockatiels (*Nymphicus hollandicus*) and ringed turtle-doves (*Streptopelia risoria*). *J. Exp. Biol.* 205:1389–409
4. Lauder GV. 2006. Locomotion. In *The Physiology of Fishes*, ed. DH Evans, JB Claiborne, pp. 3–46. Boca Raton: CRC Press. 3rd ed.
5. Lauder GV, Madden PGA, Mittal R, Dong H, Bozkurttas M. 2006. Locomotion with flexible propulsors I: experimental analysis of pectoral fin swimming in sunfish. *Bioinsp. Biomim.* 1:S25–34
6. Biewener A. 2003. *Animal Locomotion*. Oxford: Oxford Univ. Press
7. Socha JJ. 2006. Becoming airborne without legs: the kinematics of take-off in a flying snake, *Chrysopelea paradisi*. *J. Exp. Biol.* 209:3358–69
8. Jenkins FAJ. 1981. Wrist rotation in primates: a critical adaptation for brachiators. *Symp. Zool. Soc. London* 48:429–51
9. Tobalske BW, Dial KP. 2007. Aerodynamics of wing-assisted incline running in birds. *J. Exp. Biol.* 210:1742–51
10. Hedenström A, Johansson LC, Wolf M, von Busse R, Winter Y, Spedding GR. 2007. Bat flight generates complex aerodynamic tracks. *Science* 316:894–97
11. Spedding GR. 1986. The wake of a jackdaw (*Corvus monedula*) in slow flight. *J. Exp. Biol.* 125:287–307
12. Spedding G, Rosen M, Hedenström A. 2003. A family of vortex wakes generated by a thrush nightingale in free flight in a wind tunnel over its entire natural range of flight speeds. *J. Exp. Biol.* 206:2313–44
13. Dickinson MH. 1996. Unsteady mechanisms of force generation in aquatic and aerial locomotion. *Am. Zool.* 36:537–54
14. Dickinson MH, Lehmann F-O, Sane S. 1999. Wing rotation and the aerodynamic basis of insect flight. *Science* 284:1954–60
15. Vogel S. 1994. *Life in Moving Fluids. The Physical Biology of Flow*. Princeton: Princeton Univ. Press. 2nd ed.

16. Forouhar AS, Liebling M, Hickerson A, Nasiraei-Moghaddam A, Tsai H-J, et al. 2006. The embryonic vertebrate heart tube is a dynamic suction pump. *Science* 312:751–53
17. Lauder GV, Anderson EJ, Tangorra J, Madden PGA. 2007. Fish biorobotics: kinematics and hydrodynamics of self-propulsion. *J. Exp. Biol.* 210:2767–80
18. Lauder GV, Madden PGA. 2007. Fish locomotion: kinematics and hydrodynamics of flexible foil-like fins. *Exp. Fluids.* In press; doi:10.1007/s00348-007-0357-4
19. Lauder GV, Madden PGA. 2006. Learning from fish: kinematics and experimental hydrodynamics for roboticists. *Int. J. Autom. Comput.* 4:325–35
20. Dickinson M, Farley CT, Full RJ, Koehl MAR, Kram R, Lehman S. 2000. How animals move: an integrative view. *Science* 288:100–6
21. Spedding GR, DeLaurier JD. 1996. Animal and ornithopter flight. In *Handbook of Fluid Dynamics and Fluid Machinery. Vol. 3. Applications of Fluid Dynamics*, ed. JA Schetz, AE Fuhs, pp. 1951–67. New York: John Wiley
22. Bandyopadhyay PR. 2005. Trends in biorobotic autonomous undersea vehicles. *IEEE J. Oceanic Eng.* 30:109–39
23. Maybury WJ, Lehmann F-O. 2004. The fluid dynamics of flight control by kinematic phase lag variation between two robotic insect wings. *J. Exp. Biol.* 207:4707–26
24. Koditschek DE, Full RJ, Buehler M. 2004. Mechanical aspects of legged locomotion control. *Arthropod Struct. Dev.* 33:251–72
25. Weis-Fogh T. 1973. Quick estimates of flight fitness in hovering animals, including novel mechanisms for lift production. *J. Exp. Biol.* 59:169–230
26. Liem KF. 1970. Comparative functional anatomy of the Nandidae (Pisces: Teleostei). *Field. Zool.* 56:1–166
27. Fry SN, Sayaman R, Dickinson MH. 2005. The aerodynamics of hovering flight in *Drosophila*. *J. Exp. Biol.* 208:2303–18
28. Marden JH, Kramer MG. 1994. Surface-skimming stoneflies: a possible intermediate stage in insect flight evolution. *Science* 266:427–30
29. Hedrick TL, Usherwood JR, Biewener A. 2004. Wing inertia and whole-body acceleration: an analysis of instantaneous aerodynamic force production in cockatiels (*Nymphicus hollandicus*) flying across a range of speeds. *J. Exp. Biol.* 207:1689–702
30. Usherwood JR, Hedrick TL, McGowan CP, Biewener AA. 2005. Dynamic pressure maps for wings and tails of pigeons in slow, flapping flight, and their energetic implications. *J. Exp. Biol.* 208:355–69
31. Goldman JA, Koehl MAR. 2001. Fluid dynamic design of lobster olfactory organs: high speed kinematic analysis of antennule flicking by *Panulirus argus*. *Chem. Senses* 26:385–98
32. Patek S, Korff WL, Caldwell MW. 2004. Deadly strike mechanism of a mantis shrimp. *Nature* 428:819–20
33. Patek SN, Baio JE, Fisher BL, Suarez AV. 2006. Multifunctionality and mechanical origins: ballistic jaw propulsion in trap-jaw ants. *Proc. Natl. Acad. Sci. USA* 103:12787–92
34. Ahn AN, Full RJ. 2002. A motor and a brake: Two leg extensor muscles acting at the same joint manage energy differently in a running insect. *J. Exp. Biol.* 205:379–43
35. Higham TE, Day SW, Wainwright PC. 2006. Multidimensional analysis of suction feeding performance in fishes: fluid speed, acceleration, strike accuracy and the ingested volume of water. *J. Exp. Biol.* 209:2713–25
36. Day SW, Higham TE, Cheer AY, Wainwright PC. 2005. Spatial and temporal patterns of water flow generated by suction-feeding bluegill sunfish *Lepomis macrochirus* resolved by Particle Image Velocimetry. *J. Exp. Biol.* 208:2661–71

37. Westneat M. 2006. Skull biomechanics and suction feeding. In *Fish Biomechanics. Volume 23: Fish Physiology*, ed. RE Shadwick, GV Lauder, pp. 29–75. San Diego, CA: Academic
38. Gibb AC, Swanson BO, Wesp HM, Landels C, Liu C. 2006. Development of the escape response in teleost fishes: Do ontogenetic changes enable improved performance? *Physiol. Biochem. Zool.* 79:7–19
39. Goldbogen JA, Shadwick RE, Fudge DS, Gosline JM. 2005. Fast-start muscle dynamics in the rainbow trout *Oncorhynchus mykiss*: phase relationship of white muscle shortening and body curvature. *J. Exp. Biol.* 208:929–38
40. Hale M. 2002. S- and C-start escape responses of the muskellunge (*Esox masquinongy*) require alternative neuromotor mechanisms. *J. Exp. Biol.* 205:2005–16
41. Autumn K, Hsieh ST, Dudek DM, Chen J, Chitaphan C, Full RJ. 2006. Dynamics of geckos running vertically. *J. Exp. Biol.* 209:260–72
42. Tytell ED. 2006. Median fin function in bluegill sunfish, *Lepomis macrochirus*: streamwise vortex structure during steady swimming. *J. Exp. Biol.* 209:1516–34
43. Standen EM, Lauder GV. 2007. Hydrodynamic function of dorsal and anal fins in brook trout (*Salvelinus fontinalis*). *J. Exp. Biol.* 210:325–39
44. Hedrick TL, Biewener AA. 2007. Low speed maneuvering flight of the rose-breasted cockatoo (*Eolophus roseicapillus*). I. Kinematic and neuromuscular control of turning. *J. Exp. Biol.* 210:1897–911
45. Hsieh ST. 2003. Three-dimensional hindlimb kinematics of water running in the plumed basilisk lizard (*Basiliscus plumifrons*). *J. Exp. Biol.* 206:4363–77
46. Standen EM, Lauder GV. 2005. Dorsal and anal fin function in bluegill sunfish (*Lepomis macrochirus*): three-dimensional kinematics during propulsion and maneuvering. *J. Exp. Biol.* 205:2753–63
47. Stacoff A, Reinschmidt C, Nigg BM, van den Bogert AJ, Lundberg A, et al. 2001. Effects of shoe sole construction on skeletal motion during running. *Med. Sci. Sports Exerc.* 33:311–19
48. Westerweel J. 1997. Fundamentals of digital particle image velocimetry. *Meas. Sci. Technol.* V8:1379–92
49. Nogueira J, Lecuona A, Rodriguez PA. 2005. Limits on the resolution of correlation PIV iterative methods. Fundamentals. *Exp. Fluids* 39:305–13
50. Nogueira J, Lecuona A, Rodriguez PA, Alfaro JA, Acosta A. 2005. Limits on the resolution of correlation PIV iterative methods. Practical implementation and design of weighting functions. *Exp. Fluids* 39:314–21
51. Raffel M, Willert C, Kompenhans J. 1998. *Particle Image Velocimetry: A Practical Guide*. Heidelberg: Springer
52. Adrian RJ. 1991. Particle-imaging techniques for experimental fluid mechanics. *Annu. Rev. Fluid Mech.* 23:261–304
53. Lauder GV, Drucker EG. 2002. Forces, fishes, and fluids: hydrodynamic mechanisms of aquatic locomotion. *News Physiol. Sci.* 17:235–40
54. Lauder GV, Tytell ED. 2006. Hydrodynamics of undulatory propulsion. In *Fish Biomechanics. Volume 23*: *Fish Physiology*, ed. RE Shadwick, GV Lauder, pp. 425–68. San Diego, CA: Academic
55. Drucker EG, Lauder GV. 1999. Locomotor forces on a swimming fish: three-dimensional vortex wake dynamics quantified using digital particle image velocimetry. *J. Exp. Biol.* 202:2393–412
56. Tytell ED, Standen E, Lauder GV. 2008. Escaping flatland: three-dimensional kinematics and hydrodynamics of median fins in fishes. *J. Exp. Biol.* In press

57. Danos N, Lauder GV. 2007. The ontogeny of fin function during routine turns in zebrafish (*Danio rerio*). *J. Exp. Biol.* 210:3374–86
58. Walker JA. 1998. Estimating velocities and accelerations of animal locomotion: a simulation experiment comparing numerical differentiation algorithms. *J. Exp. Biol.* 201:981–95
59. Harper DG, Blake RW. 1989. On the error involved in high-speed film when used to evaluate maximum accelerations of fish. *Can. J. Zool.* 67:1929–36
60. Daley MA, Felix G, Biewener AA. 2007. Running stability is enhanced by a proximo-distal gradient in joint neuromechanical control. *J. Exp. Biol.* 210:383–94
61. Roberts TJ, Scales JA. 2004. Adjusting muscle function to demand: joint work during acceleration in wild turkeys. *J. Exp. Biol.* 207:4165–74
62. Mittal R, Dong H, Bozkurttas M, Lauder GV, Madden PGA. 2006. Locomotion with flexible propulsors II: computational modeling and analysis of pectoral fin swimming in sunfish. *Bioinsp. Biomim.* 1:S35–41
63. Sane S, Dickinson MH. 2002. The aerodynamic effects of wing rotation and a revised quasi-steady model of flapping flight. *J. Exp. Biol.* 205:1087–96
64. Walker JA, Westneat M. 2002. Kinematics, dynamics, and energetics of rowing and flapping propulsion in fishes. *Int. Comp. Biol.* 42:1032–43
65. McHenry MJ, Azizi E, Strother JA. 2003. The hydrodynamics of locomotion at intermediate Reynolds numbers: undulatory swimming in ascidian larvae (*Botrylloides* sp.). *J. Exp. Biol.* 206:327–43
66. Pontzer H, Lieberman DE, Momin E, Devlin MJ, Polk JD, et al. 2006. Trabecular bone in the bird knee responds with high sensitivity to changes in load orientation. *J. Exp. Biol.* 209:57–65
67. Usherwood JR, Williams SB, Wilson AM. 2007. Mechanics of dog walking compared with a passive, stiff-limbed, 4-bar linkage model, and their collisional implications. *J. Exp. Biol.* 210:533–40
68. Wilson AM, McGuigan MP, Su A, van den Bogert AJ. 2001. Horses damp the spring in their step. *Nature* 414:895–99
69. Gatesy SM, Middleton K, Jenkins FA, Shubin NH. 1999. Three-dimensional preservation of foot movements in Triassic theropod dinosaurs. *Nature* 399:141–44
70. Baier DB, Gatesy SM, Jenkins FA. 2007. A critical ligamentous mechanism in the evolution of avian flight. *Nature* 445:307–10
71. Wilga CD, Lauder GV. 2002. Function of the heterocercal tail in sharks: quantitative wake dynamics during steady horizontal swimming and vertical maneuvering. *J. Exp. Biol.* 205:2365–74
72. Nauen JC, Lauder GV. 2002. Hydrodynamics of caudal fin locomotion by chub mackerel, *Scomber japonicus* (Scombridae). *J. Exp. Biol.* 205:1709–24
73. Drucker EG, Lauder GV. 2002. Experimental hydrodynamics of fish locomotion: functional insights from wake visualization. *Int. Comp. Biol.* 42:243–57
74. Drucker EG, Lauder GV. 2003. Function of pectoral fins in rainbow trout: behavioral repertoire and hydrodynamic forces. *J. Exp. Biol.* 206:813–26
75. Hedenström A, Rosen M, Spedding G. 2006. Vortex wakes generated by robins *Erithacus rubecula* during free flight in a wind tunnel. *J. R. Soc. Interface* 3:263–76
76. Dabiri JO, Colin SP, Costello JH. 2006. Fast-swimming hydromedusae exploit velar kinematics to form an optimal vortex wake. *J. Exp. Biol.* 209:2025–33
77. Nauen JC, Lauder GV. 2002. Quantification of the wake of rainbow trout (*Oncorhynchus mykiss*) using three-dimensional stereoscopic digital particle image velocimetry. *J. Exp. Biol.* 205:3271–79

78. Lindken R, Westerweel J, Wieneke B. 2006. Stereoscopic micro particle image velocimetry. *Exp. Fluids* 41:161–71
79. Hoyer K, Holzner M, Lüthi B, Guala M, Liberzon A, Kinzelbach W. 2005. 3D scanning particle tracking velocimetry. *Exp. Fluids* 39:923–34
80. Hanke W, Brucker C, Bleckmann H. 2000. The ageing of the low-frequency water disturbances caused by swimming goldfish and its possible relevance to prey detection. *J. Exp. Biol.* 203:1193–200
81. Spedding GR. 2003. Comparing fluid mechanics models with experimental data. *Philos. Trans. R. Soc. London Ser. B* 358:1567–76
82. Gharib M, Pereira F, Dabiri D, Hove JR, Modarress D. 2002. Quantative flow visualization: toward a comprehensive flow diagnostic tool. *Int. Comp. Biol.* 42:964–70
83. Adrian RJ. 1997. Dynamic ranges of velocity and spatial resolution of particle image velocimetry. *Meas. Sci. Technol.* 8:1393–98
84. Peng J, Dabiri JO, Madden PG, Lauder GV. 2007. Non-invasive measurement of instantaneous forces during aquatic locomotion: a case study of the bluegill sunfish pectoral fin. *J. Exp. Biol.* 210:685–98
85. Dabiri JO. 2005. On the estimation of swimming and flying forces from wake measurements. *J. Exp. Biol.* 208:3519–32
86. Yen J. 2000. Life in transition: balancing inertial and viscous forces by planktonic copepods. *Biol. Bull.* 198:213–24
87. Catton KB, Webster DR, Brown J, Yen J. 2007. Quantitative analysis of tethered and free-swimming copepodid flow fields. *J. Exp. Biol.* 210:299–310
88. Birch JM, Dickinson MH. 2001. Span-wise flow and the attachment of the leading edge vortex on insect wings. *Nature* 412:729–33
89. Drucker EG, Lauder GV. 2005. Locomotor function of the dorsal fin in rainbow trout: kinematic patterns and hydrodynamic forces. *J. Exp. Biol.* 208:4479–94
90. Drucker EG, Lauder GV. 2000. A hydrodynamic analysis of fish swimming speed: wake structure and locomotor force in slow and fast labriform swimmers. *J. Exp. Biol.* 203:2379–93
91. Drucker EG, Lauder GV. 2001. Wake dynamics and fluid forces of turning maneuvers in sunfish. *J. Exp. Biol.* 204:431–42
92. Hanke W, Bleckmann H. 2004. The hydrodynamic trails of *Lepomis gibbosus* (Centrarchidae), *Colomesus psittacus* (Tetraodontidae) and *Thysochromis ansorgii* (Cichlidae) investigated with scanning particle image velocimetry. *J. Exp. Biol.* 207:1585–96
93. Nauen JC, Lauder GV. 2001. Locomotion in scombrid fishes: visualization of flow around the caudal peduncle and finlets of the chub mackerel *Scomber japonicus*. *J. Exp. Biol.* 204:2251–63
94. Sane SP. 2006. Induced airflow in flying insects. I. A theoretical model of the induced flow. *J. Exp. Biol.* 209:32–42
95. Sane SP, Jacobson NP. 2006. Induced airflow in flying insects. II. Measurement of induced flow. *J. Exp. Biol.* 209:43–56
96. Dickinson M. 2001. Solving the mystery of insect flight. *Sci. Am.* 284:49–57
97. Elsinga GE, Scarano F, Wieneke B, van Oudheusden BW. 2006. Tomographic particle image velocimetry. *Exp. Fluids* V41:933–47
98. Pereira F, Gharib M. 2002. Defocusing digital particle image velocimetry and the three-dimensional characterization of two-phase flows. *Meas. Sci. Technol.* 13:683–94
99. Tobalske BW, Warrick DR, Clark CJ, Powers DR, Hedrick TL, et al. 2007. Three-dimensional kinematics of hummingbird flight. *J. Exp. Biol.* 210:2368–82

100. Lauder GV. 1983. Functional and morphological bases of trophic specialization in sunfishes. *J. Morphol.* 178:1–21
101. Liem KF. 1984. The muscular basis of aquatic and aerial ventilation in the air-breathing teleost fish *Channa*. *J. Exp. Biol.* 113:1–18
102. Van Wassenbergh S, Herrel A, Adriaens D, Aerts P. 2007. Interspecific variation in sternohyoideus muscle morphology in clariid catfishes: functional implications for suction feeding. *J. Morphol.* 268:232–42
103. Brainerd E, Liem KF, Samper C. 1989. Air ventilation by recoil aspiration in polypterid fishes. *Science* 246:1593–95
104. Brainerd EL. 1994. Pufferfish inflation: functional morphology of postcranial structures in *Diodon holocanthus* (Tetraodontiformes). *J. Morphol.* 220:243–61
105. Socha JJ, Westneat MW, Harrison JF, Waters JS, Lee WK. 2007. Real-time phase-contrast x-ray imaging: a new technique for the study of animal form and function. *BioMed. Cent. Biol.* 5:1–6
106. Westneat MW, Betz O, Blob RW, Fezzaa K, Cooper WJ, Lee WK. 2003. Tracheal respiration in insects visualized with synchrotron X-ray imaging. *Science* 299:558–59
107. Harper DG, Blake RW. 1989. A critical analysis of the use of high-speed film to determine maximum accelerations of fish. *J. Exp. Biol.* 142:465–71